HAL open science

Ammonia and ethanol blend as fuel for ICE: from the liquid injection to the combustion and pollutant emissions

Ronan Pelé, Pierre Brequigny, Jérôme Bellettre, Camille Hespel, Guillaume Dayma, Fabien Halter, Christine Mounaïm-Rousselle

To cite this version:

Ronan Pelé, Pierre Brequigny, Jérôme Bellettre, Camille Hespel, Guillaume Dayma, et al.. Ammonia and ethanol blend as fuel for ICE: from the liquid injection to the combustion and pollutant emissions. Twentieth International Conference on Flow Dynamics, Nov 2023, Sendai, Japan. hal-04403091

HAL Id: hal-04403091

https://hal.science/hal-04403091v1

Submitted on 18 Jan 2024

HAL is a multi-disciplinary open access archive for the deposit and dissemination of scientific research documents, whether they are published or not. The documents may come from teaching and research institutions in France or abroad, or from public or private research centers.

L'archive ouverte pluridisciplinaire **HAL**, est destinée au dépôt et à la diffusion de documents scientifiques de niveau recherche, publiés ou non, émanant des établissements d'enseignement et de recherche français ou étrangers, des laboratoires publics ou privés.

Distributed under a Creative Commons Attribution - NonCommercial - NoDerivatives 4.0 International License

Ammonia and ethanol blend as fuel for ICE: from the liquid injection to the combustion and pollutant emissions

Ronan Pelé[1], Pierre Brequigny[1], Jérome Bellettre[2], Camille Hespel[1], Guillaume Dayma[3], Fabien Halter[3], Christine Mounïam-Rousselle[1]
[1]Univ. Orléans, INSA CVL, EA 4229 - PRISME, F-45072 Orléans, France
[2]LTeN UMR CNRS 6607, Université de Nantes, 1 rue Christian Pauc, CS 50609, 44306 Nantes Cedex 3, France
[3]Univ. Orléans, CNRS-ICARE, Orléans, France

ABSTRACT

This study aims to provide full knowledge about the different steps to optimize ammonia/ethanol blends as fuel for Spark-Ignition engine in terms of injection, laminar flame speed, engine performances and pollutant emissions. From the experimental study of the liquid spray of different ammonia/ethanol blends, at low air density, it was concluded that the spray shapes are correlated to the Liquid-Vapor equilibrium diagram. Sprays located in the liquid region in the diagram have similar weak plumes-to-plumes interactions due to slow vaporization and a liquid phase state. For the liquid-vapor region, a transient phase is observed and, when the vapor region is reached, plumes-to-plumes interaction is stronger with a collapsing effect due to a drop of the temperature inside the spray creating a low-pressure zone. From the experimental study of laminar flame speed, using two spherical expanding flame techniques under constant pressure and volume conditions, it was concluded that the addition of 25% of ethanol doubles the laminar flame speed of ammonia and enhances its reactivity. Last by performing experiments in Spark ignition engine, as a function of liquid blend direct injection strategy, it was concluded that high stability is obtained whatever the content of ethanol in the blends. Even if for pure ammonia it was also possible, the operating conditions are more restrictive for pure ammonia. The thermal efficiency is improved in the case of 75% of ethanol in the blend but with consequence on NOx emissions. It can be concluded that trade-offs between performances and pollutant emissions have to be addressed for ammonia/ethanol blends as a function of ammonia and ethanol availabilities.

1. Introduction

To mitigate climate challenges, switching to carbon-free fuels such as hydrogen and ammonia are highlighted to be interesting solutions to decarbonizing energy, transport, and industrial sectors, especially by considering their production from water electrolysis with green electricity. Hydrogen is an attractive energy carrier [1] but its storage and transport issues, its low ignition energy, and very wide flammability range are the main drawbacks to safety [2]. Ammonia, containing 17.8% by weight of hydrogen, can be stored in the liquid phase at approximately 9 bar at 20°C or -34°C at ambient pressure. Its high auto-ignition temperature and research octane number (RON=130), narrow flammability range, and low laminar flame speed [3] make its combustion challenging. The use of ammonia in compression ignition engines is limited by its properties, and mainly by its high autoignition temperature, one of the key parameters of these engines. Nonetheless, in these difficult ignition conditions, the help of a spark can be useful as in [9,10] and has the advantage to optimize combustion by controlling the ignition time. But, as consequence, improve the ammonia reactivity by adding a supplementary fuel, i.e. a promoter, is an interesting way.

Biofuels are highlighted as another alternative energy source with low global warming impact. Bio-ethanol remains the most attractive one [4]. It can be produced from a wide variety of sources such as starch, sugarcane, lignocellulosic material derived from agricultural waste, and algae [5] reducing its CO_2 footprint. Therefore, the idea here is to consider bio-ethanol as combustion improver for ammonia due to its higher reactivity. The total solubility of ammonia in liquid ethanol is due to the polarities of both molecules [6] and their vapor-liquid equilibrium was determined experimentally [7,8]. Consequently, the homogeneous liquid ammonia/ethanol can be directly used as a classic liquid fuel and injected directly into the internal combustion chamber.

The injection process is a key aspect to optimize local air/fuel ratio inside the combustion chamber, which affects the pollutant emission itself [11]. The advantage of direct injection compared to port fuel is not only to help the filling of the engine but also to vaporize as fast as possible the fuel inside the chamber by breaking up the fuel spray into droplets. Then, the vaporization of droplets is greatly significant for the spatial distribution of fuel vapor/air, the ignition, and the combustion itself. Generally, the use of high-pressure injection systems [12] favors the atomization in small droplets which enhances the liquid-air interface, the vaporization, and the fuel/air mixing [13,14]. The effects of injection pressure on droplet size reduction become limited or even disappear when the injection pressure reaches a threshold [12]. Another possibility to reduce droplet size is the flash boiling condition itself, which produces finer droplets and a more uniform fuel/air mixture [12]. Flash boiling is a thermodynamic state of fuel spray that occurs when a subcooled liquid is rapidly depressurized to a pressure below its liquid saturation pressure [15].

Adding ethanol into ammonia generates an "effervescent-like" atomization due to their high difference in vapor pressures: $P^{Sat}_{C_2H_5OH}(293K) = 5.4kPa$ and $P^{Sat}_{NH_3}(293K) = 855.8kPa$, [16][17] thus potentially improving the ethanol vaporization when the pressure is below the saturation pressure of ammonia during the direct injection.

When an air/vapor fuel mixture is ignited by means of

Corresponding author: Ronan Pelé
E-mail address: ronan.pele@univ-orleans.fr

a spark, the laminar flame speed is one major property that drives the combustion process. The knowledge of the laminar flame speed is required to understand the burning behavior of an air/fuel mixture especially in the case of blend as ammonia/ethanol. It is also one key parameter to improve the validity of kinetic mechanisms, useful for accurate CFD simulations to design new systems.

This study aims to provide knowledge about the behavior of ammonia/ethanol blends in terms of injection, laminar flame speed and engine performances, and pollutant emissions.

2. Injection study

2.1 Vapor-Liquid Equilibrium

The ratio of the saturation pressure to the ambient pressure, commonly called Rp, is a classical criterion to identify the flash boiling condition for pure fuel; Rp>1 means flash boiling condition. However, for a binary fuel, the use of the LVE diagram is essential to identify the regions with or without flash boiling. The phase state of the mixture is calculated with the equation of the state of Peng-Robison using the full methodology described in [18]. The calculations are then validated against experimental data. The bubble and dew point curves are determined for the mixture at the experimental conditions delimiting three regions: only vapor, vapor, and liquid and only liquid. The only vapor region is considered as the flash boiling zone, the vapor and liquid as a transition regime, and the only liquid as a "classic" regime.

2.2 Methods

A constant volume 2.5 L chamber was used to follow the spray development fully described in [19]. Between each spray, the chamber is purged with flushed air that is vented to the outside. All the different blends are pressurized up to 120 bar by pressurized Helium. A current gasoline direct Bosch injector (7 holes of 150 µm diameter and its reference number is 0261500494) is used to generate the spray. The temperature and injection duration are controlled through an automation system driven by a Labview program. The pressure and the temperature are measured by a pressure sensor from Keller (PAA-33X model) and a T thermocouple with a precision of ±4 mbar and ±0.1 K respectively.

The Schlieren technique was used to capture images of liquid spray and is fully described in [16]. The images are recorded at 15,000 frames per second with a Cmos high-speed camera (FastCam SA5, Photron), associated with a 105 mm Nikkon camera lens, to reach an image resolution of 768 × 648 pixels^2, with a spatial resolution of 0.160 mm/pixel. For each operating condition, 10 repetitions were done with 100 images recorded. Shutter time is set to 1/147000 second.

The experimental data presented in this study correspond to different conditions of ambient pressures, temperatures, and air densities as defined in [16]. The injection pressure, P_{fuel}, was set at 120 bar and the injection temperature, T_{fuel}, was considered maintained at the ambient temperature, i.e 20°C, as there is no thermocouple in the injector nozzle. The injection timing is set at 4ms to characterize the spray morphology. Four ratios of ammonia/ethanol (25%, 50%, 75%, and 90% of NH_3 by mole defined as X25, X50, X75, and X90) are compared to pure fuels. They are prepared in the liquid phase thanks to a mixing set-up using an emulsifier already used in [20].

2.3 Results and Discussion

Figure 1 shows the raw spray images after 1 ms of injection for the different ratios of ammonia at $P_{ambient}$=2bar and $T_{ambient}$=293K. The spray of pure ethanol, and X25, are similar and some of the individual plumes are distinguishably meaning few interactions between them. These weak interactions are mainly due to the liquid state of these mixtures thus meaning a slow

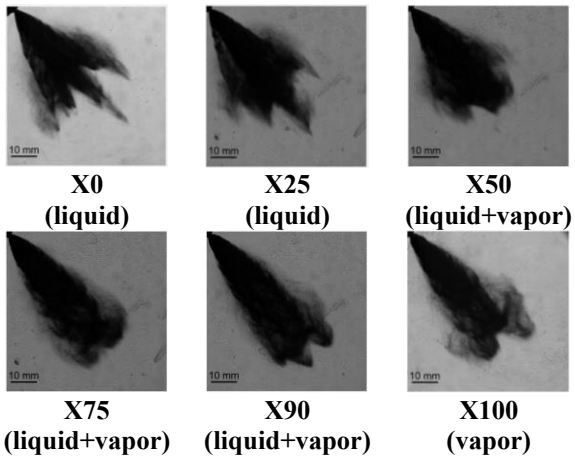

Fig. 1 Comparison of spray shape at 1 ms after the start of injection obtained for the different ratio of ammonia at $P_{ambient}$=2bar and $T_{ambient}$=293K, P_{inj} =120bar. The region phase from the calculation is indicated in the brackets.

vaporization process. On the contrary, for the image which corresponds to the vapor phase, the spray is very thin and collapsed with a strong plumes-to-plumes interaction. The individual plumes are not visible due to the rapid vaporization. This rapid state change decreases quickly the temperature inside the global spray creating a low-pressure region inside and the plumes get closer. Between these two opposite spray morphologies, the 'transient' spray morphologies are observed. For the ratio X50 at 20°C, the individual plumes are not visible but the sprays are not collapsed as the spray is large. It can be explained by the fact that ammonia vaporizes at first but the decrease in the temperature inside the spray is not enough cold to collapse the spray. However, when more ammonia is added to the blend, X75 and X90 at 20°C, the spray collapses with a strong interaction between plumes probably due to the colder temperature inside the spray because of a higher amount of ammonia vaporized. The spray shapes are correlated to the liquid-vapor equilibrium calculation.

3. Laminar flame speed

3.1 Methods

The full methodology for the spherical expanding

flame techniques under constant pressure is fully described in [21] as the experimental data. The constant volume spherical flame method is employed in this study to determine the laminar flame speed of blends of ammonia and ethanol. This method allows the measurement of the laminar flame speed of expanding spherical flames by using both pressure and flame radius growth [22]. This method relies on the hypothesis of an isentropic compression of the unburned gases following the ignition: thus, resulting in a simultaneous increase of both pressure and temperature within the vessel. Therefore, each flame propagation is submitted to pressure, and temperature simultaneously increase thus giving flame speed values as a function of the couple (P, T). A pressure transducer records the change in pressure, whereas the temperature change is calculated for each pressure using Laplace's law. Flame chemiluminescence visualization was adopted to obtain the radius evolution by means of a CMOS camera (PHANTOM V1611). Images were captured at an adapted rate of 5 000 fps for ammonia only and up to 15 000 fps for ethanol only due to the laminar flame speed difference.

The experiments were done for different stoichiometric blends of ammonia/ethanol and, the initial pressure P_0 is set at 1 and 2 bar and the initial temperature T_0 is fixed at 423.15 K for each blend, enabling to process data up to 650 K and 10 bar.

3.1 Results and Discussion

The isobaric measurement [21] showed an increase in the reaction with the addition of ethanol. The addition of 25% of ethanol doubles the laminar flame speed of ammonia and enhances the reactivity of ammonia.

Figure 2 illustrates the isentropic evolution of the laminar flame speed as a function of (P,T) simultaneously from an initial unburned condition (T_0, P_0). The laminar flame speed, y-axis, is plotted for the couples (P,T) with a split x-axis, on the left: the temperature trace and, on the right: the pressure trace. The simultaneous increase of both pressure and temperature within the vessel due to the isentropic compression increases the laminar flame speed. A horizontal line on the y-axis determines (P,T) conditions of the measurement of the laminar flame speed. The thick traces represent the laminar flame speed including the experimental uncertainty of 5% as described above and consistent with [23]. A greyscale from black to grey as a function of the ethanol content increase in the blend (black corresponds to ammonia and the lightest grey to ethanol) was used and the non-linearity is also remarked for the high-pressure conditions. The pure ammonia (X100) reactivity is correctly reproduced with Shrestha-PCRL the merged mechanism while the prediction from CEU mechanism are the lowest. The merge mechanism Shrestha-PCRL is based on the oxidation mechanism from Shrestha optimized for ammonia only. Consequently, the laminar flame speed is not well reproduced for the high content of ethanol (X0 and X25). On the contrary, the CEU mechanism agrees with the high-pressure data but is slightly low for pure ethanol (X0) and X25 and overestimates the isobaric data by 7 $cm.s^{-1}$ for X0. For the blends X75 and X50, the CEU mechanism is in very good agreement with isochoric results performed at 1 bar of initial pressure.

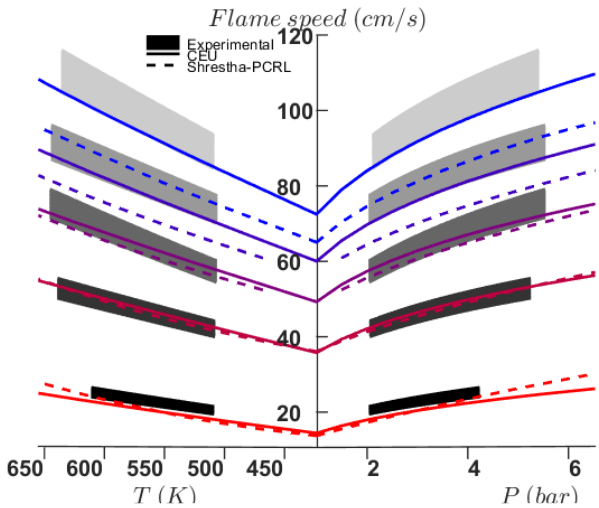

Fig. 2 Comparison of predicted laminar flame speed with 2 kinetic mechanisms to experimental values for ammonia/ethanol blends; Experimental values: Thichened line colored with a grey scale; the different line styles correspond to the laminar flame speed simulated with several mechanisms (blue for ethanol and red for ammonia) for P_0=1 bar and T_0=423.15 K.

4. Engine performance and pollutants emissions

All the experiments of this section and the methodology are described in [24]**.** The Lower Heating Value (LVH) of the blend decreased slowly up to X50 and few change of the mass injected is needed to maintain the constant energy input. However, for higher ammonia ratio, the LHV decreases strongly due to the high difference between LHV of ethanol and ammonia. Compensation by more fuel is necessary to increase the fuel energy and target the same indicated mean effective pressure (IMEP). The change of combustion durations with the ammonia content increases mainly due to the decrease of laminar flame speed with ammonia content, -41% and -86% from pure ethanol to X50 and pure ammonia respectively, at ignition conditions, with CEU mechanism previously validated with the laminar flame speed data. The thermal efficiency, Figure 3, has the same behaviour as the combustion efficiency and up to 40.5% for X25, providing good performances and a positive effect of ammonia by considering ethanol as the main fuel. Unburnt NH_3 emission, Figure 5.a, increases as a function of the ammonia content with the highest value for pure ammonia as slightly rich fuel/air mixture was needed to stabilize the combustion. In terms of NOx, the behaviour is non-linear with ethanol amount in the blend as a maximum value 4 times higher than in the case of pure ethanol and obtained for X50. It could be concluded that lean equivalence ratio for all blends and even pure ethanol are favourable conditions when considering NOx formation. As expected, some increases of NOx are obtained as a function of NH_3 quantity. The same trend was observed for methane/ammonia [25,26] with a

maximal NO emission for a 50/50 blend. NOx emissions for pure ammonia are lower by 12% than for pure ethanol, mainly due to an equivalence ratio a bit higher than the stoichiometry.

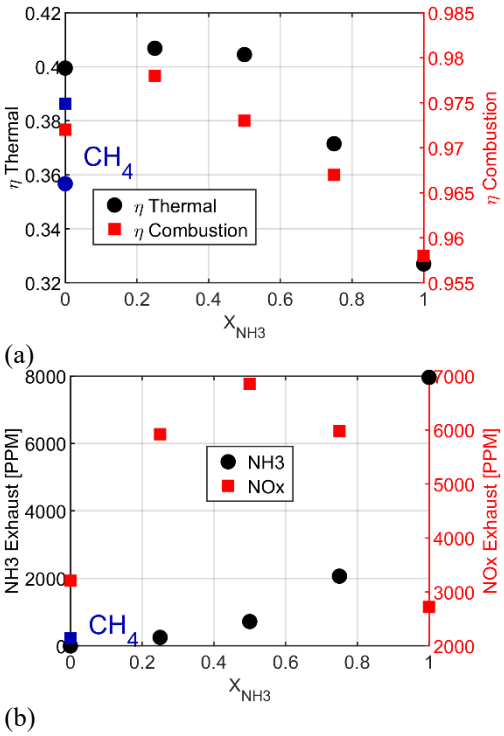

Fig. 3 Variation of (a) thermal and combustion efficiencies and (b) pollutant emissions: NH_3 and NOx as a function of the ethanol/ammonia blends at 1 bar of intake pressure and homogeneous condition

5. Concluding Remarks

The potential of ammonia/ethanol blend as fuel for Direct Injection Spark Ignition Engine was investigated from the injection behavior to the combustion to the engine performances.

1-The spray morphologies during injection process are correlated to the vapor-liquid equilibrium. A spray located in the liquid phase region from the LVE diagram is larger with few plumes to plume interaction while for pure ammonia in vapor phase, flash boiling effect appears.

2-The addition of ethanol to ammonia can enhance sufficiently the reactivity of ammonia as the laminar flame speed is doubled with only 25% of ethanol in ammonia/ethanol blend. CEU mechanism predicts well the experimental data obtained.

3-Not only ethanol is an improver of ammonia engine but ammonia is also an improver of ethanol engine as the thermal efficiency is enhanced by adding 25% of NH_3 when ethanol is the main fuel. Therefore, the addition of ammonia could be also one possibility to help to decarbonize engines running with biofuels. NOx emissions reached the highest value for 50/50 blend and as expected, unburnt NH_3 emissions can increase with the increase of ammonia addition in the blend. Some tradeoffs can be obtained and active control can help to ensure full post-treatment.

Acknowledgments

The research leading to these results has received funding from the French Government's "Investissement d'Avenir" program: "Laboratoire d'Excellence CAPRYSSES" (Grant No ANR-11- LABX-0006-01)

References

[1] V.T. Sacramento EM, Carvalho P, Lima LC, Energy Pol (2013).

[2] Y. Li, M. Bi, B. Li, Y. Zhou, L. Huang, W. Gao, Energy 159 (2018) 252–263.

[3] C. Lhuillier, P. Brequigny, F. Contino, C. Mounaïm-Rousselle, Fuel 269 (2020) 117448.

[4] A. Katoch, A. Millán-Merino, S. Kumar, Fuel 231 (2018) 37–44.

[5] C.C. Geddes, I.U. Nieves, L.O. Ingram, Curr. Opin. Biotechnol. 22 (2011) 312–319.

[6] M.C. Rehbein, C. Meier, P. Eilts, S. Scholl, Energy and Fuels (2019).

[7] L.J. Huang, W.L. Xue, Z.X. Zeng, Fluid Phase Equilib. 303 (2011) 80–84.

[8] Z.X. Zeng, J. Chen, W.L. Xue, L.J. Huang, Ind. Eng. Chem. Res. 50 (2011) 3592–3597.

[9] C. Mounaïm-Rousselle, P. Bréquigny, C. Dumand, S. Houillé, Energies 14 (2021) 1–13.

[10] A. Mercier, C. Mounaïm-rousselle, P. Brequigny, J. Bouriot, C. Dumand, 11 (2022) 1–9.

[11] A. Montanaro, L. Allocca, Combust. Sci. Technol. 191 (2019) 1600–1608.

[12] M. Xu, Y. Zhang, W. Zeng, G. Zhang, M. Zhang, SAE Int. J. Fuels Lubr. 6 (2013) 137–148.

[13] M. Chang, Z. Lee, S. Park, S. Park, Fuel 271 (2020) 117600.

[14] J.D. Naber, D.L. Siebers, SAE Tech. Pap. (1996).

[15] M. Chang, J. Hwan Park, H. Ik Kim, S. Park, Appl. Therm. Eng. 170 (2020) 114969.

[16] R. Pelé, C. Mounaïm-Rousselle, P. Bréquigny, C. Hespel, J. Bellettre, Fuels 2 (2021) 253–271.

[17] E. Tinon, Etude Expérimentale Des Mécanismes d'atomisation Effervescente. Application à La Sécurité Incendie Dans Les Moteurs Aéronautiques, UNIVERSITÉ DE TOULOUSE, 2018.

[18] R. Privat, J.N. Jaubert, Y. Privat, Comput. Chem. Eng. 50 (2013) 139–151.

[19] J. Dernotte, (2012) 261.

[20] Y. Ji, J. Bellettre, A. Montillet, P. Massoli, Int. J. Multiph. Flow 131 (2020) 103402.

[21] R. Pelé, P. Brequigny, C. Mounaim-Rousselle, G. Dayma, F. Halter, Fuel Commun. 10 (2022) 100052.

[22] F. Halter, Z. Chen, G. Dayma, C. Bariki, Y. Wang, P. Dagaut, C. Chauveau, Combust. Flame 212 (2020) 165–176.

[23] A. Karan, G. Dayma, C. Chauveau, F. Halter, Combust. Flame 236 (2022) 111819.

[24] R. Pelé, P. Brequigny, J. Bellettre, C. Mounaïm-rousselle, R. Pelé, P. Brequigny, J. Bellettre, C.M. Performances, Int. J. Engine Res. (2023) 1–14.

[25] H. Xiao, A. Valera-Medina, P.J. Bowen, Energy 140 (2017) 125–135.
[26] G. Battista, G. Sorrentino, R. Ragucci, M. De, P. Sabia, 241 (2022).